**EduVision: Journal of Innovations in Pedagogy and Educational Advancements**
**Volume 01, Issue 08, August, 2025**
brightmindpublishing.com
**ISSN (E): 3061-6972**


# MULTIFACTOR EXPERIMENT, EXPERIMENTAL RESULTS AND DEVELOPMENT OF REGRESSION EQUATIONS IN WELDING AND APPLICATION OF COATINGS ON EXCAVATOR BUCKET TEETH

Zulfikorov Dostonbek Rustamjon ogly,
Andijan State Technical Institute , Uzbekistan

**Abstract**

The results of testing some types of alloys revealed the potential of using metastable austenitic wear-resistant alloys to strengthen the working parts of excavator bucket teeth. However, alloys 55X7 G7T and 100X6 Alloys G6S3FAP, the alloys selected as prototypes for optimization have shortcomings that determine the need for further work on optimizing the composition of the coating material. Alloy 55X7 G7T has unsatisfactory strength characteristics. Active phase-bound kinetics leads to an increase in resistance to microscratching , but does not contribute to the preservation of the plastic resource under additional impact-abrasive effects. Optimization should be carried out in the direction of obtaining stretched kinetics with the preservation of residual austenite due to the carbon content in the solid solution. To improve wear resistance without reducing the strength properties, an increase in the amount of the carbide phase can be achieved, as indicated above, by replacing chromium carbides with finely dispersed special VC carbides in a vanadium alloy. An additional reserve is the introduction of calcium silicate into the surfacing process for grinding and orienting the dendritic structure and increasing the number of aligned crystals. A positive example of the use of calcium silicon as a modifier in coatings for flux-cored wire welding can be seen in [ 1].

**Keywords**: Excavator, bucket, tooth, protective element, efficiency, trouble-free operation, reliability, rock, abrasive wear, hard coating, coating, weld seam.

## Introduction

Alloy 100X6 G 6 C3 FAP is characterized by a complex alloying system without a base. For the initial strengthening of carbides, it is necessary to limit alloying with vanadium, and it is recommended to exclude boron, since additional strengthening

EduVision: Journal of Innovations in Pedagogy and Educational Advancements
Volume 01, Issue 08, August, 2025
brightmindpublishing.com
ISSN (E): 3061-6972


with borides leads to embrittlement of the alloy without significantly increasing its corrosion resistance. Alloying with nitrogen can be carried out using a plasma-forming gas containing nitrogen [2]. The silicon content in the alloy requires adjustment. On the one hand, it displaces carbon from the solid solution, which contributes to the destabilization of austenite and acceleration of the kinetics *y - a* - transformations, as well as an increase in the amount of carbide phase. On the other hand, it embrittles the solid solution, and also increases the tendency to thermal cracking during welding and surfacing.

Based on the results of alloy test analysis, tasks were set to develop a filler flux-cored wire for PCW of the working part of excavator bucket teeth, obtained using the apparatus of the theory of planning extreme experiments to optimize the chemical composition of the metal of chromium-manganese metastable austenite with additional alloying with vanadium and silicon and modification with silicocalcium . The main requirements for the base metal were maximum wear resistance achieved in the micro-scratching mode with additional impact-abrasive action, in combination with sufficient strength properties. One of the important parameters is the compatibility of the base and deposited metals. Minimal use of vanadium as an alloying element was one of the solutions in implementing the task.

**Methods definitions parameters optimization**

The value of the relative specific work of micro-scratching after impact-abrasive action εм 1 , determined by the above method, was chosen as the main parameter for optimizing Y 1 in the course of a multifactorial experiment. Since the production of small lots of experimental flux-cored wires is associated with significant difficulties, the experimental alloys were made from 110G13L steel samples using a PP AN-106 (PP 10 X 14 T) plasma arc, obtained by hardening with the addition of flux-cored wire. The composition of the deposited coating contained 5-7% of the chromium source. In the course of the multifactorial experiment, the parameters of the hardening mode were maintained constant to obtain a weld bead 18 mm wide and 20 mm deep. The PQYO modes correspond to Table 1.2. In this case, the manganese content was 7-9%. Additional alloying of the molten metal bath was carried out by plasma-arc remelting of a ceramic rod of rectangular cross-section 10x5 mm, consisting of ferroalloy and graphite powders, bound with liquid glass as an electrode coating. The values of crack initiation deformations and

EduVision: Journal of Innovations in Pedagogy and Educational Advancements
Volume 01, Issue 08, August, 2025
brightmindpublishing.com
ISSN (E): 3061-6972


destructive stresses during fragmentation were used as control parameters for optimization Y 2 and Y 3 , respectively.

**Method for determining crack initiation stress**

One of the most important quality criteria for wear-resistant surfacing coatings is crack resistance. Evaluation of the tendency to crack formation, both from residual stresses and from external loads, is the starting point for designing a rational technology for obtaining surfacing coatings, allows predicting their behavior both during production and during operation, and significantly accelerates the search for an optimal solution.

As for testing wear-resistant coating materials, there are several methods for assessing crack resistance based on assessing the behavior of the deposited coating layer during plastic bending or determining the number of certain energy effects required to form cracks in the deposited layer [2]. The first method cannot be considered correct, since it is somewhat subjective and does not allow for identifying differences between alloys with similar properties. In addition, under special operating conditions, bending with plastic deformation is extremely rare, and negative behavior of the material during plastic bending is not yet a reason for its rejection.

The second method (VNIST test) provides valuable information on resistance to crack formation under low-cycle dynamic loading. However, its main drawbacks are the requirements for the size of the samples and the lack of information on the forces that lead to crack formation. Therefore, the criterion for evaluating the tests of samples using the VNIST method is comparative .

The most preferred criterion for crack resistance is the true critical stress or crack initiation strain. This criterion is absolute, since it allows comparison and control of previously obtained results using other methods.

To determine the mechanical properties of metals under dynamic loads, in particular deformation at the onset of crack formation, impact bending tests with oscillography of the signal from a strain gauge attached to the impactor of a pile driver are widely used [4], in which the impact load of the impactor can be accurately estimated from the oscillogram when cracks appear based on a characteristic fracture . The magnitude of the critical load on the impactor determines the forces that will destroy the sample. This method gives satisfactory

EduVision: Journal of Innovations in Pedagogy and Educational Advancements
Volume 01, Issue 08, August, 2025
brightmindpublishing.com
ISSN (E): 3061-6972


reproducible results for standard-sized samples made of homogeneous materials. Inhomogeneous samples obtained by applying coatings are characterized by sensitive fluctuations in the geometric dimensions and chemical composition of the surface coatings. This significantly increases the spread of experimental data in the indirect determination of destructive forces.

The method of direct measurement of crack initiation deformations in coated specimens using strain gauges ( strain sensors ) attached to bare metal in the crack initiation zone [3] is free of the disadvantages inherent in indirect testing methods using oscillography . Specimens are tested for cantilever deflection by applying a single impact without free fall of the load. In all cases, the impact energy must be sufficient to initiate a crack already at the first impact. Scheme tests presented in Figure 1, a.

A wear-resistant metal coating layer 2 is welded on. Strain gauge 2 is oriented with resistance along the line of action of normal bending stresses and is attached to the welded coating layer in the area where a crack may occur.

Next, the strain gauge is connected to the strain gauge bridge according to the structural diagram shown in Figure 1b, after which the bridge is balanced. To calibrate the measuring path, the control imbalance Uk is determined by connecting the control imbalance resistance Rk » Rd parallel to the tested sensor with resistance Rd .

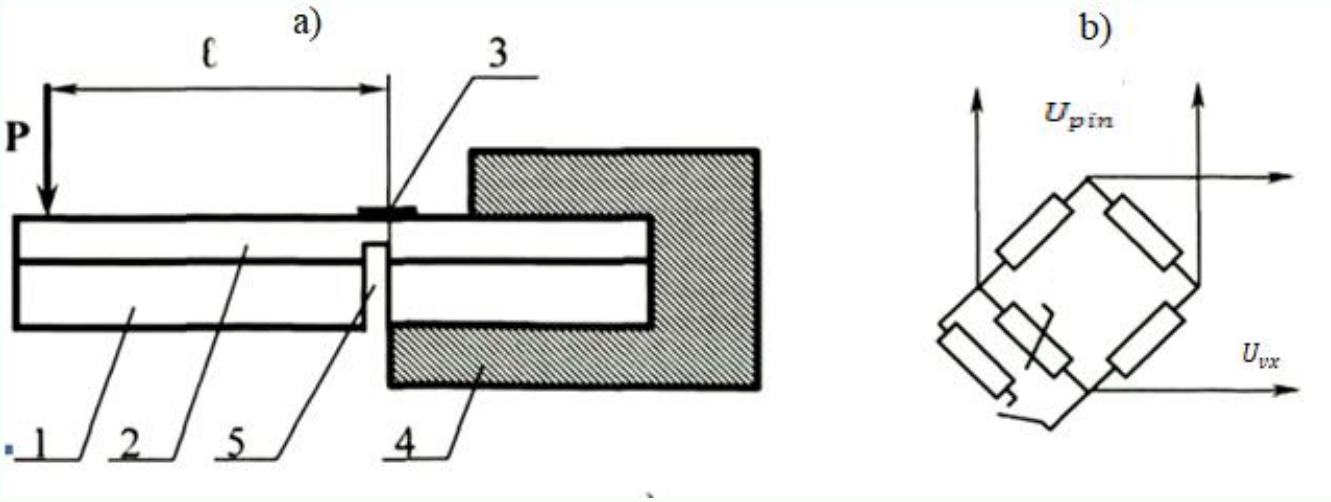


Fig. 1. Determination of deformation at the beginning of a crack [ 4 ] .
*a* - research scheme , *b* - diagram of a deformation bridge

EduVision: Journal of Innovations in Pedagogy and Educational Advancements
Volume 01, Issue 08, August, 2025
brightmindpublishing.com
ISSN (E): 3061-6972


The sample is placed in clamp 4 and a load of force *P is applied to the free end of the sample* . The energy of the impact force must be sufficient to cause a crack. For large sample sizes, a special cut 5 is made under the coated metal layer. The signal from the strain gauge is amplified by an amplifier and recorded on the screen of a storage oscilloscope (Fig. 1, b ) . The moment of crack occurrence corresponds to a break in the oscillogram . Crack occurrence strain $\varepsilon_{et}$ proportional to the stress at the crack point $U_{et}$ and is determined by the following formula.

$$\varepsilon_{3T} = \frac{U_{3T} \cdot R_D}{U_K (R_K + R_D) \cdot K} \quad (1)$$

Where : K is the strain gauge sensitivity coefficient specified in the strain gauge data sheet .

$\varepsilon_{3t}$ was chosen as the optimization criterion *Y 5* .

**Weld delamination test procedure**

The tests of the welded seams of the samples were carried out similarly to the " Implant " method [6], which is used in tests for the tendency to form cold cracks and is distinguished by its exceptional simplicity and acceptable reliability. Scheme preparations The samples for testing are presented in Figure 2.

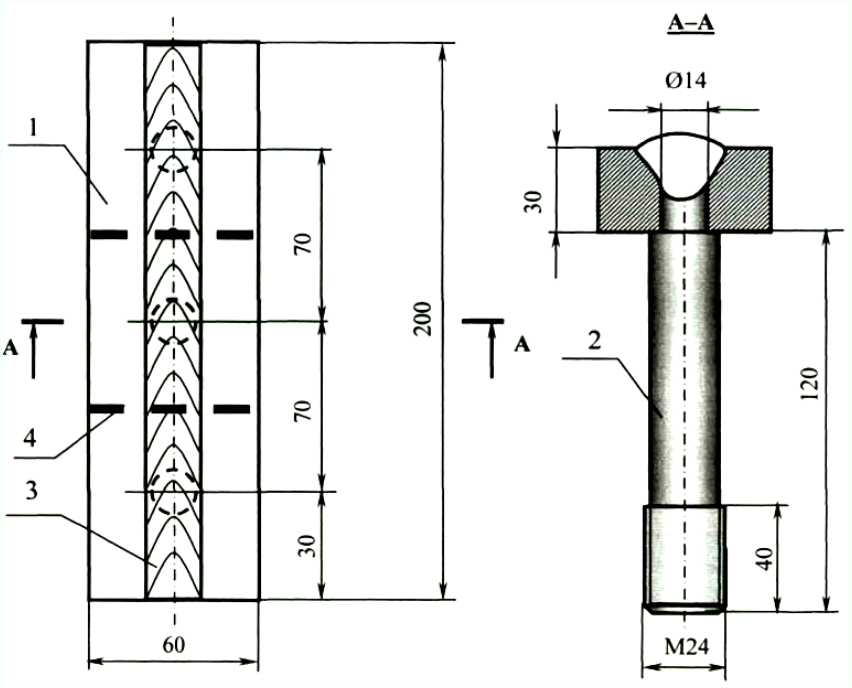


Fig. 2. Sample prepared for welding seam

EduVision: Journal of Innovations in Pedagogy and Educational Advancements
Volume 01, Issue 08, August, 2025
brightmindpublishing.com
ISSN (E): 3061-6972


The tests were carried out in the following sequence. In the working part of *the* $P_{o}$ $_{6n}$ *in* three parts 1 with a diameter of 8 mm, three holes with a cross-sectional area of 2 were drilled. The core and plates were made of 110G13L steel. To obtain satisfactory machinability, the blanks were annealed at a high temperature of 650 °C. After mechanical processing, the parts were quenched at a temperature of 1050 °C. Three-roller rollers were welded to the upper edge of the plate , and a welded joint was formed between the core and the plate. After this, the plate was cut into $_{4}$ parts by punching, samples were made for tensile testing and the breaking load R was determined . The criterion for the resistance of the welded seam *Y 3* was the tensile strength *σ ism* = P / F (GPa).

## Experiment results

### Construction of regression equations

The multifactorial experiment is presented in the diagram shown in Figure 3. To assess the dispersion of the experiment, experiment No. 1 was repeated 4 times. The obtained data were recorded in worksheets.

$$Y_1 \cdot 10^{-1}, \frac{Y_2}{\%}, \frac{Y_3}{\Gamma\Pi A}$$

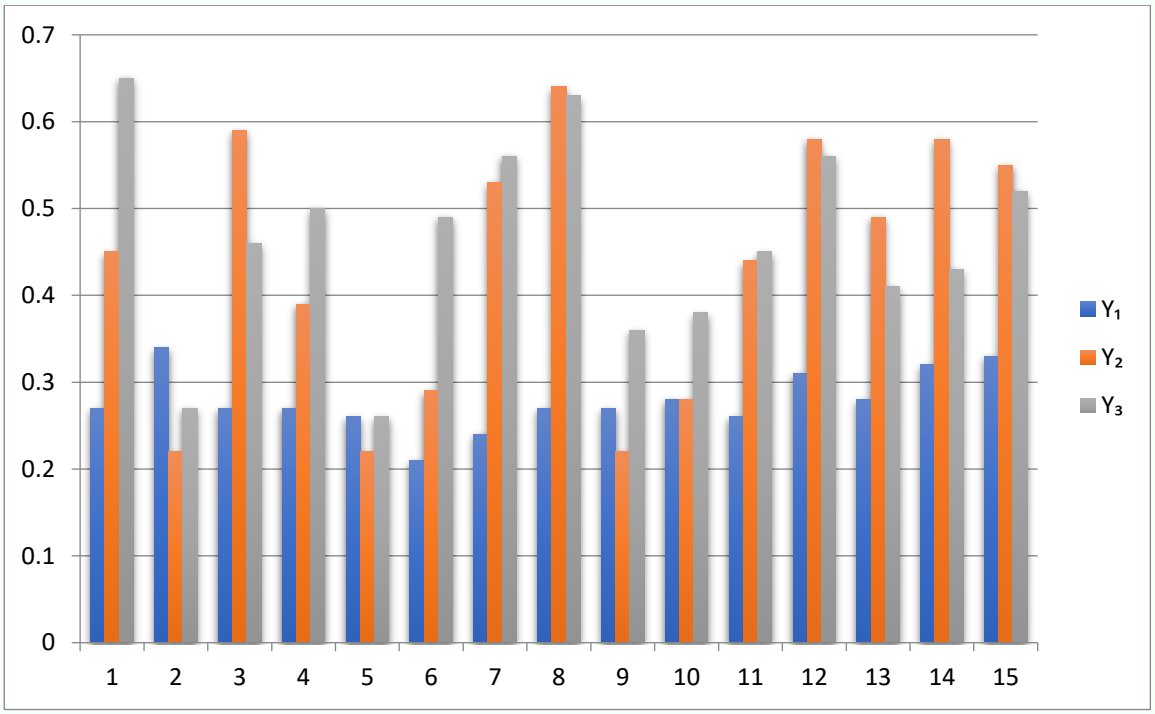


Fig. 3. Diagram of the results of the multifactorial experiment.

EduVision: Journal of Innovations in Pedagogy and Educational Advancements
Volume 01, Issue 08, August, 2025
brightmindpublishing.com
ISSN (E): 3061-6972


The following regression equations were obtained : Relative erosion resistance
$Y_1 = 3.1 + 0.06 X_2 - 0.402 X_2^2 - 0.103 X_3 + 0.201 X_4 + 0.175 X_2 X_3 + 0.13 X_3 X_4$.
Crack initiation deformation $Y_1$, %
$Y_2 = 0.621 + 0.054 X , 0.112 X_2 - 0.011 X_3 + 0.030 X_4 - 0.94 X , ^2 - 0.093 X_4^2 - 0.014 X_3 X_4$.
Weld seam delamination stress , MPa
$Y_3 = 537.5 - 95.2 \times_2 - 56.1 \times_3 - 38.2 \times_4$
From them it turns out that silicon and vanadium can be used in food against mostbigeffect shows . Silicon, displacing carbon from austenite, promotes the formation of additional $Y_1$carbides and the intensification of *the* $\gamma$ - *a* transformation. With an increase in the silicon content, wear resistance first increases, reaches a maximum, and then decreases, which is explained by an increase in the brittleness of the α - martens site. Vanadium forms finely dispersed carbides and nitrides. The source of nitrogen in the coated metal is a plasma-forming gas containing nitrogen. Additions of all alloying elements in the studied factor space negatively affect the resistance of the weld to delamination. The crack initiation deformation increases with an increase in the silicon and vanadium content within certain limits and decreases with an increase in the carbon and silicon content. The addition of silica and calcium has a positive effect on the strength properties of the coated metal and has an obvious modifying effect.
The results of the analysis of the obtained models showed that in order to achieve the best values of individual optimization parameters, it is necessary to change the factors in different directions. To solve the compromise problem, a generalized acceptability function was used as a complex optimization parameter .

**Calculation of the acceptability function**

Acceptability function $d_1$; varies in the range 0–1.0 for the first optimization parameter. The acceptability scale is constructed as follows [7]:
$d_1 = 1.0$ - the maximum achievable level of quality, in most cases unknown, and its achievement is not always necessary;
0.8 -1.0 - a very high level of quality, which does not always need to be achieved;
0.6 -1.0 - good quality level (slightly higher than what can actually be achieved);
0.37 -0.6 - sufficient quality level;

EduVision: Journal of Innovations in Pedagogy and Educational Advancements
Volume 01, Issue 08, August, 2025
brightmindpublishing.com
ISSN (E): 3061-6972


0.37 - specified quality level;
0 -0.37 - unacceptable quality level.
The values of the specified value of the optimization parameter *Yi* are determined in the following sequence.
d are installed and assigned ik acceptable levels of $Y_{i2}$ and unacceptable levels $Y_{i1}$ *(control points)* . values corresponding to the required scale;
Dimensionless parameters are determined by the following formula [8].

$$y_{tk}^{t} = -\ln\ln\frac{1}{d_{ik}} \quad (2)$$

Using the equation of a straight line passing through two points, known from analytical geometry, a linear functional dependence *y ' ¡ ( Yi ) is established:*

$$\frac{y_i^t - y_{i1}^t}{y_{i2}^t - y_{i1}^t} = \frac{Y_1 - Y_{i1}}{Y_{i2} - Y_{i1}} \quad (3)$$

Equation (1.2) calculates the values of $y'$ .
$d_i$The values are calculated using the formula

$$d_i = e^{-(e^{-y_i^t})} \quad (4)$$

After finding the desirability functions for all optimization parameters, the overall desirability function *D* is found as the geometric mean of the known desirability functions for all experiments.

$$D = \sqrt[n]{\prod_{i=1}^{n} d_i} \quad (5)$$

Reliable points

**Table 1**

| Code | Yes | member | y' |
|---|---|---|---|
| $Y_{11}$<br>$Y_{12}$ | 2.0<br>4.0 | 0.2<br>0.8 | -0.47588<br>1.49994 |
| $_{21}$ years old<br>$Y_{22}$ | 0.2<br>0.7 | 0.2<br>0.7 | -0.47588<br>1.03093 |
| $_{31}$ years old<br>$Y_{32}$ | 0.4<br>0.65 | 0.37<br>0.6 | 0.00576<br>0.67172 |

EduVision: Journal of Innovations in Pedagogy and Educational Advancements
Volume 01, Issue 08, August, 2025
brightmindpublishing.com
ISSN (E): 3061-6972


Figure 4 shows a nomogram for converting *Y values.* $_i$ into the corresponding values of the desired function *d* .

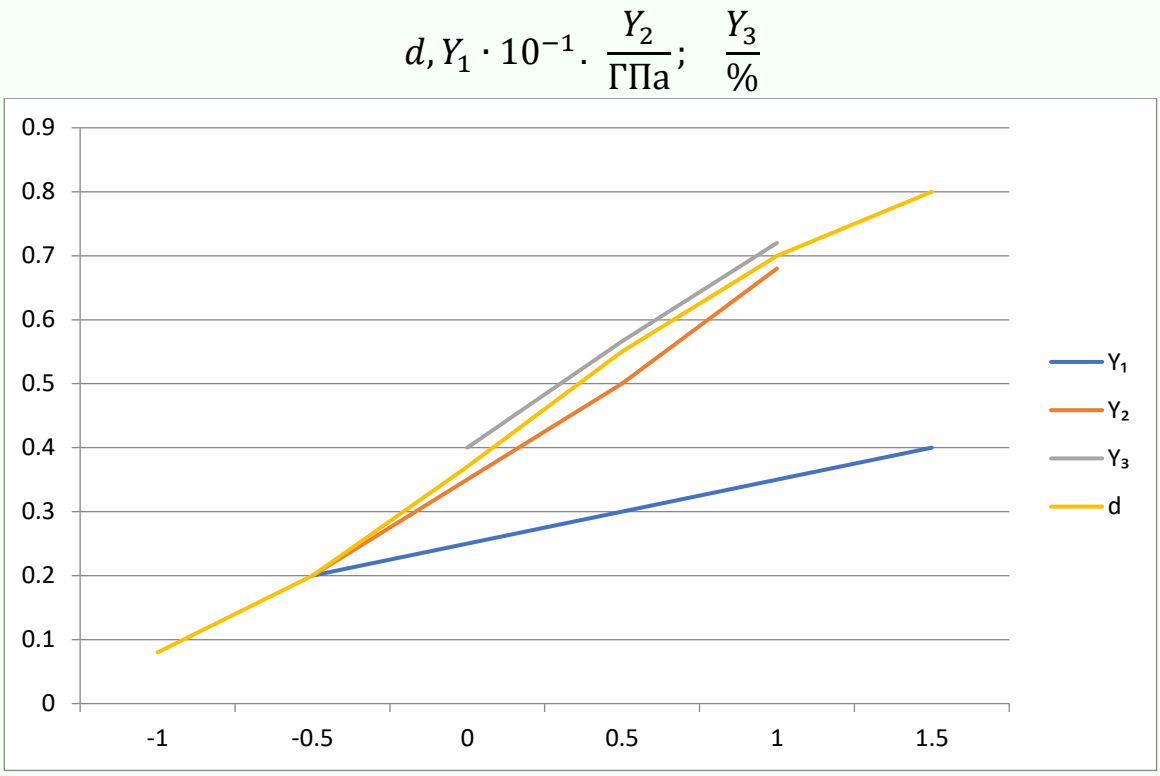


Fig. 4. Nomogram for calculating the values of *d* ( $_{Yi}$)

The results of calculating the generalized and partial feasibility functions for all optimization parameters of the multivariate experiment are presented in Appendix 4. The values of *D obtained for each experiment* were substituted into the worksheet from which the linear regression equation for *D was calculated.* , the coefficients of which have the form [12].

$D = 0.5749 + 0.0188 X_1 - 0.0668 X_2 + 0.0219 X_4 - 0.0145 X_3 X_4$ . (6)

### 1.4. Powdered wire account

PQYO technological process of automation of the deposited metal layer known chemical composition, providing the required working output of powdered wire. Electrode metal is diluted with the base metal taking into account the combination obtained without taking into account, in table 1 the composition of the powdered wire is given, the content of the main and alloying elements, disappearing taking into account the obtained in the case if alloying with manganese is provided by the

EduVision: Journal of Innovations in Pedagogy and Educational Advancements
Volume 01, Issue 08, August, 2025
brightmindpublishing.com
ISSN (E): 3061-6972


base metal.
The calculations were carried out according to the methodology presented in the literature [9].

Table 2 Chemical composition of flux-cored wire

| Number of elements M, % | | | | | |
|---|---|---|---|---|---|
| WITH | Kr | Ca | IN | Si | Na2SiF6 |
| 1.7 | 14 | 2 | 5.0 | 5.0 | 0.8 |

1. We determine the required quantity of alloy components $P_i$ (except graphite) and the quantity of carbon introduced by them $C_i$ per 100 g of wire:

$$P_i = \frac{a_i \cdot 100}{b_i};\ C_i = \frac{P_i \cdot c_i}{100},\ (7)$$

where $a$ is the required amount of the element, %
$b_i$ - the amount of the element in this component, %
$c_i$ - carbon content in this component, %
$c$, required to obtain a given amount of carbon $a$, is determined by the formula.

$$P_C = \frac{(a_c - \sum_{i=1}^{n} C_i) \cdot 100}{b_c} \qquad (8)$$

where $b_c$ — carbon content in graphite, %.

2. We determine the sum of the masses of the components $\Sigma P_i$ ( taking into account the amount of graphite and sodium fluorosilicate $Na_2SiF_6$)
3. The sum of the volumes of all components is determined by the ratio $\Sigma P_i / \rho_{ni}$, where $\rho_{ni}$ - the mass density of the 1st component, which is related to the density of the monolithic material by the ratio $p_i$.
$\rho_{ni} = k * \rho_i$
by [ 10], $k$ =0.56-0.6; in most cases $k$ =0.59.
The calculation results are presented in Table 3.

**EduVision: Journal of Innovations in Pedagogy and Educational Advancements**
**Volume 01, Issue 08, August, 2025**
brightmindpublishing.com
**ISSN (E): 3061-6972**


Table 3 The amount of alloying components per 100 g of flux-cored wire

| | Number of elements,% | | | | | *Pi and* G | *WITH* G | $p_i/p_{ni}$ cm $^3$ |
|---|---|---|---|---|---|---|---|---|
| | *Ca* | *Si* | *Kr* | *IN* | *WITH* | | | |
| Silicocalcium SK15 | 15 | 45 | - | - | 0.2 | 13.33 | 0.026 | 2,119 |
| Ferrochrome FH100 | - | - | 65.0 | - | 1.0 | 21.54 | 0.215 | 5,318 |
| Ferrovanadium VD-1 | - | 2.0 | - | 35.0 | 0.75 | 14.29 | 0.086 | 2,484 |
| Graphite ZT | - | - | - | - | 90.0 | 1.43 | - | 1.85 |
| Ferrosilicon FS 50 | - | 50 | - | - | - | - | - | - |
| Na2SiF6 | - | - | - | - | - | 0.6 | - | - |
| | | | | general | | 61.2 | 0.414 | 11.78 |

$F$ is determined $_{o\,b}$ shells and $F_{sh}$

$$f = \frac{F_{ob}}{F_{\text{ш}}} = \frac{100 - \sum P_i}{p_{ob} K_y K_B \sum {}^{P_i}/_{p_{ni}}} = 0.62; \qquad (9)$$

where $\rho_{ob}$ – density of the shell metal;

$K_y$ - coefficient taking into account the charge compression when winding with tape ( $K_y$ = 0.95 - 0.97);

$K_v$ is the permeability coefficient, which depends on the difference in granulation of the components (with the same granulation of all components $K_v$ = 1, with different granulation $K_v$ = ( 0.80-0.95) and is determined by the experimental curve [10].

Wire diameters $d$ *are selected* $_{np}$ = 2.6 mm and winding pattern $d_n$ = (1.5- 1 ,7) $d_n$ p = 4.0 mm.

According to empirical formulas taken from [9], the dimensions of a strip of 08kp steel are determined provided that there is no iron powder in the charge:

Tape width

$$b = \pi d_B = 12{,}4 \approx 12{,}0mm \qquad (10)$$

Tape thickness

$$\delta = 0{,}55 d_B \left(1 - \sqrt{\frac{1}{1+f}}\right) = 0{,}47 \approx 0{,}5mm \qquad (11)$$

## Conclusions

The mechanism of the influence of gas-phase transformation on the formation of the primary structure of eutectic alloys has been revealed. It consists in eliminating and improving the orientation of the columnar primary structure and increasing the

EduVision: Journal of Innovations in Pedagogy and Educational Advancements
Volume 01, Issue 08, August, 2025
brightmindpublishing.com
ISSN (E): 3061-6972


number of equiaxed crystallites. An alloy with an optimal composition of the surface coating of the 130Kh6G8S2AF2 type has been obtained and a powder wire for applying the coating by plasma and auxiliary arcs has been developed. The microstructure of the coated metal is dendrites of metastable austenite in lediburite , and carbon nitride precipitates are also located throughout the volume of the dendrites [12] . The alloy has a high sensitivity to phase hardening and is well compatible with the base metal. The parameters of the welding mode for excavator bucket teeth have been optimized for plasma and auxiliary arc welding , which makes it possible to achieve a hardening depth of up to 20 mm with defect-free formation of wear-resistant rollers [13]. Production tests of welded coated teeth of quarry excavator buckets have shown high durability. The use of the developed technology allows increasing the durability of excavator bucket teeth by 1.7–1.9 times. As a result of multifactorial experiments, the optimal alloy composition for strengthening the working surfaces of quarry excavator bucket teeth was obtained. Optimization was carried out according to three optimization parameters using the proportionality function when solving a compromise problem and the steepest ascent method when passing to the optimal region. The PP-170Kh14S5F5 powder wire has been developed, intended for alloying a metal bath when strengthening excavator bucket teeth and other parts made of 110G13L steel using the plasma and auxiliary electric arc method.

**References**

1. ЛюбичА.И.Влияниесиликокальциевые структурыплавленного металла / А.И.Любич , А.Б.Пустовгар // Сварочноепроизводство . 2002. №6. Стр . 46-47.
2. ЛившисЛ . С ., ГринбергН . А ., КуркумеллиН . Г . Основылегированиянаплавленногометалла / Л . С . Лившис , Н . А . Гринберг , Н. Г . Куркумелли . М .: Машиностроение , 1969. 187 стр .
3. Воротников , В.Я. Методика определения устойчивости плавочных сплавов к ударнымнагрузкам / В.Я.Воротников , С.В.Иванов , Ю.А. Артеменко // Автоматическая сварка. 1983. № 9. С. 61 - 62.
4. Венсис . Оценка инерциальнойнагрузкиприударномтестанисос иллографированием / С. Венси , А. Приест , М. Май //Сб. « Ударныетестанияметаллов ». М.: Мир, 1973. Стр. 157-174.

EduVision: Journal of Innovations in Pedagogy and Educational Advancements
Volume 01, Issue 08, August, 2025
brightmindpublishing.com
ISSN (E): 3061-6972


5. ПокъодняИ.К.Газивсварныхшвах / И.К.Покъодня . М.: Машиностроение, 1972. 256 стр.
6. МакаровЭЛ . М.: Машиностроение, 1981. 247 стр.
7. ПетровГ.Л.Сварочныйматериал / ГЛПетров // Л.: Машиностроение; 1972. 280 стр .
8. Рустамджоногли З.Д. АНАЛИЗ ТЕХНОЛОГИИ ВОССТАНОВЛЕНИЯ ЗУБЬЕВ КОВШЕЙ ЭКСКАВАТОРА // ТВОРЧЕСКИЙ УЧИТЕЛЬ.– 2023. – Т.3. – № 34. – С.179-182.
9. Рустамджоноглу З.Д. МЕТОДИКА МОДЕЛИРОВАНИЯ ПЕРВИЧНОЙ КРИСТАЛЛИЗАЦИИ ЗУБЬЕВ КОВША ЭКСКАВАТОРА // Новости образования : исследования в XXI веке .- 2024.- Т. 2.– № 20. - Стр . 255-262.
10. ХашимовХ . Х. Обоснование противоабразивной износостойкости зубьев ковшей экскаваторов, эксплуатируемых в нашей республике // Образовательные исследования в области общечеловеческих наук. – 2023.– Т. 2.– № 1 СПЕЦ. – С. 386-391.
11 .Мамажонов З.А. АНАЛИЗ СОВЕРШЕНСТВОВАНИЯ МЕТОДОВ ВОССТАНОВЛЕНИЯ ЗУБЬЕВ КОВШЕЙ ЭКСКАВАТОРОВ, ЭКСПЛУАТИРУЕМЫХ В НАШЕЙ РЕСПУБЛИКЕ //МЕЖДУНАРОДНЫЕ КОНФЕРЕНЦИИ.– 2023. – Т.1. – №2.– С. 482-487.
12. Anvar, Djurayev, Odilov Khayrullo, and Zulfiqorov Dostonbek. "DETERMINING THE SPECIFIC VIBRATION FREQUENCY OF A PIECE OF COTTON ON A DRUM WITH A TOOTHED BELT." Universum: технические науки 8.4 (133) (2025): 22-25.
13. Qodirov, Ziyodulla, Dostonbek Zulfiqorov, and Baxramali Iminov. "Tut ipak qurti pillalarini chuvishga tayyorlashning takomillashtirilgan texnologiyasi." MUHANDISLIK VA IQTISODIYOT 2.4 (2024).